Differential Stress in MgO Measured in the Deformation-DIA by Using High-resolution Monochromatic Diffraction

T. Uchida, Y. Wang, M.L. Rivers, S.R. Sutton
Consortium for Advanced Radiation Sources (CARS), The University of Chicago, Chicago, IL, U.S.A.

Introduction

Measurements of the room-temperature yield strength of MgO at high pressures have been attempted intensively in the past decade (see Ref. 1 for a review). Various experimental techniques have been used in determining the high-pressure strength of polycrystalline MgO, including measuring the radial distribution of pressure and the final sample thickness in a diamond anvil cell (DAC) [2], peak breadth of x-ray diffraction in a conventional DIA [3], and distortion of the Debye rings recorded parallel to the loading axis in a DAC [1]. In all of these previous studies, differential stress is not an independent experimental parameter; rather, it is a consequence of either a pressure gradient or an elasticity mismatch at grain-to-grain level, neither of which can be controlled. Because of the inability to vary differential stress, one cannot demonstrate convincingly that the sample has reached its yield point, nor can one specify the dependence of yield strength on total sample strain.

In the present study, we report on results from differential stress measurements in MgO up to 6 GPa at room temperature from using the newly developed deformation-DIA (D-DIA) [4] by monochromatic diffraction with a 2-D charge-coupled device (CCD) detector. We used sintered polycrystalline cubic boron nitride (cBN) anvils that are x-ray transparent; thus, we were able to collect complete Debye rings (with the entire 360° azimuth coverage) with a 2θ range up to about 12°. By using high-energy x-rays (small wavelengths), diffraction lines down to about 1 Å can be recorded within this 2θ range. Ellipticity of the Debye rings provided information on elastic lattice distortions due to the differential stress. Detailed procedures were developed in obtaining differential stress from the lattice strain measurement, based on lattice strain theory [5]. We demonstrated that by advancing/retracting the differential rams, differential stress levels in the sample could be controlled under a given pressure and temperature condition. This capability allowed us to examine correlations of certain experimental observables with the differential stress level.

Methods and Materials

Figure 1 shows schematic configuration of the entire setup (top view). The D-DIA module [4] is compressed in the 250-ton press [6] installed at GSECARS beamline station 13-BM-D [7] at the APS. As the differential rams of the D-DIA advance (retract) the sample, the top and bottom anvils push toward (retreat from) the sample, causing the main hydraulic ram load to increase (decrease). Therefore, an additional hydraulic ram is tapped into the main ram for fine adjustments in main ram load, in order to maintain a constant pressure.

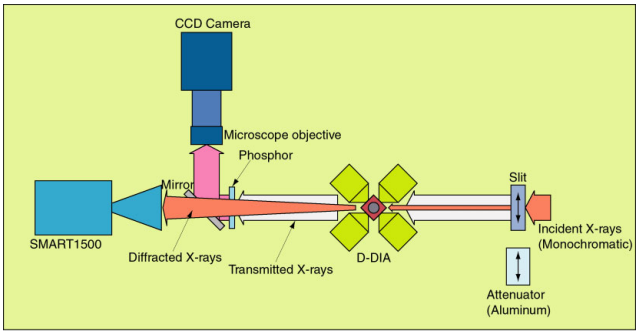

FIG. 1. Schematic illustration of x-ray diffraction and imaging setup (top view). Transmitted x-rays are converted by the YAG single-crystal phosphor to visible light, which is then reflected by the mirror through the microscope objective into the MicroMax CCD camera. For the imaging mode, the YAG and mirror assembly is in the beam path, and the incident slits are out of it. For the x-ray diffraction, incident slits are moved in, and both the CCD camera and YAG assemblies are moved out from the beam path. Diffracted x-rays travel above the YAG assembly and are detected by a Bruker SMART 1500 CCD detector. A monochromatic beam of 55.0 keV (λ = 0.225 Å) is used for both imaging and diffraction.

A monochromatic x-ray beam (55.0 keV, corresponding to a wavelength of 0.225 Å) with an overall beam size of about 3 × 3 mm is used. For diffraction, the incident x-rays were collimated to 200 × 200 μm by two pairs of tungsten carbide entrance slits, and the diffracted x-rays were detected by a Bruker SMART 1500 x-ray CCD detector (1024 × 1024 pixels). An x-ray imaging system was mounted on the press frame to monitor the sample during compression and ram advancement/retraction cycles. Radiographic imaging was accomplished by retracting the entrance slits from the x-ray path and by projecting the x-ray absorption contrast of the high-pressure cell assembly onto a

yttrium-aluminum-garnet (YAG) phosphor, which converted x-rays to visible light that was viewed by a MicroMax CCD camera (1300×1000 pixels) through a microscope objective. By using a 5× objective, an area of 2.6×2.0 mm^2 could be observed, with a resolution of 2 μm/pixel throughout the runs.

A powdered MgO sample was sandwiched by sintered Al_2O_3 pistons in a 6-mm edge-length cube made of a mixture of amorphous boron and epoxy resin.

Prior to an experiment, the tilt and rotation of the SMART 1500 relative to the incident x-ray beam were calibrated with an x-ray diffraction standard (CeO_2). We used the sample diffraction pattern at ambient conditions to determine the sample-to-detector distance. At each pressure, differential rams were advanced at a constant speed to shorten the sample, while diffraction patterns and x-ray images were repeatedly recorded at 300-s and 60-s exposures at the center of the sample, respectively.

Two experiments were conducted, each with two deformation cycles at two different pressures. In the first run, pressure was increased to 2 GPa, and the differential rams were advanced by 0.4 mm in total displacement (0.2 mm for each ram). The pressure was then increased to 6 GPa, where the differential rams were advanced by another 0.5 mm. Finally the ram load was released. In the second run, pressure was first increased to 5 GPa, and both rams were advanced by 0.35 mm. Then the pressure was decreased to 1.5 GPa, followed by another 0.4-mm ram advancement, after which the main ram load was released.

Results

Figure 2 shows the lattice distortion for the (*200*) reflection obtained from x-ray diffraction as a function of azimuth. During the first deformation cycle in the first run at 2 GPa, distortion of the Debye ring (*200*) increased, as indicated by the increasing magnitude of sinusoidal modulation. After the first deformation cycle, the sample was compressed isotropically to 6 GPa, between data sets 036 and 039. During the second deformation cycle at 6 GPa, distortion of the (*200*) Debye ring was further increased. Note that at the magic angle $\varphi = 35.26°$, lattice strain remained almost constant, especially at 6 GPa, indicating that we were successful in maintaining a constant pressure. After the run, the lattice strain returned to zero (data set 063). Despite having different compression and deformation histories, the second run showed quite similar distortion (Fig. 2, bottom).

One of the critical issues in measuring the yield strength of materials by using diffraction is how to detect yielding. In the D-DIA, total strain measurement is essential in establishing reproducible stress-strain curves (Fig. 3). Complications may arise, however, if the sample has high porosity. Our data indicate that a powdered sample is not desirable in deformation experiments (Fig. 3, run 1, path 1). In the first deformation cycle at 2 GPa in run 1, the strain rate of the MgO sample was about twice as fast as that of the other three cycles, whereas we advanced differential rams with a constant rate for all four deformation cycles. The slope is shallower than that of other three cycles by a factor of about 2 (Fig. 3). Total strains determined by using the imaging technique may be compromised by the presence of pores, which, depending on their geometry, may require extremely high pressures to close. Fully densified starting materials would be much more desirable.

Yield strength measurements of MgO from using different techniques are summarized in Fig. 4 [1-3, 8-10], together with our results. Note that only in the D-DIA can differential stress be independently controlled at a given pressure.

Our differential stress data lie between the upper bound [1, 8, 9] and the lower bound [2]. Meade and Jeanloz [2] noted that their assumptions might cause an underestimate of the yield strength; therefore, their data provided a lower bound. Although our elastic anisotropy data suggest sample yielding (at least in [*100*]), we consider that we might not reach yielding for the entire sample. Only the last data point is therefore shown (in solid symbols), indicating the lower bound of yield strength.

Weidner et al. [3] relied on grain-to-grain stress heterogeneity to deform the crystallites. It is difficult to determine whether the sample has yielded. Their sample is compressed by zirconia end plugs in a conventional DIA. We observe that in our experiments, isotropic compression did not cause a significant accumulation of differential stress (Fig. 2). Merkel et al. [1] used a DAC with essentially the same analytical method as ours. The initial difference in our stresses and Merkel et al.'s [1] stresses indicates the difference in the magnitude of nonhydrostaticity between the DAC and the D-DIA. As we advance differential rams, the magnitude of nonhydrostaticity becomes greater and higher, so differential stress is approaching that in the DAC.

MgO has widely been employed as a pressure standard. In the same way, we planned to use this material as a "piezometer" to measure stress and apply the stress data to the sample adjacent to the piezometer. When MgO yielded, we observed some anomalies in anisotropy. Further careful experiments and discussion are needed in order to apply the stress data to the sample.

Discussion

Differential stress levels in the sample could be controlled successfully under a given pressure and temperature condition during deformation cycles (Figs. 2 and 3). This capability allowed us to examine correlations of certain experimental observables with the differential stress level.

Acknowledgments

We thank N. Lazarz, F. Sopron, M. Jagger, G. Shen, M. Newville, P. Eng, J. Pluth, P. Murray, and C. Pullins for their valuable contributions. To convert 2-D diffraction data into "cake" form, the program FIT2D was used. We express our thanks to A. Hammersley and European Synchrotron Radiation Facility (ESRF) personnel for the public use of FIT2D. We thank W. Durham for use of the D-DIA. We also thank S. Merkel for discussion. This work was performed at the GSECARS beamline at the APS. GSECARS is supported by the National Science Foundation (Earth Sciences), U.S. Department of Energy (DOE, Geosciences), W.M. Keck Foundation, and U.S. Department of Agriculture. Use of the APS was supported by the DOE Office of Science, Office of Basic Energy Sciences, under Contract No. W-31-109-ENG-38.

References

[1] S. Merkel, H.R. Wenk, J. Shu, G. Shen, P. Gillet, H.K. Mao, and R.J. Hemley, J. Geophys. Res. **107**(11), 2271 (2002).

[2] C. Meade and R. Jeanloz, J. Geophys. Res. **93**, 3261-3269 (1988).

[3] D.J. Weidner, Y. Wang, and M.T. Vaughan, Geophys. Res. Lett. **21**, 753-756 (1994).

[4] W. Wang, W.B. Durham, I.C. Getting, and D.J. Weidner, Rev. Sci. Instrum. **74**, 3002-3011 (2003).

[5] A.K. Singh, J. Appl. Phys. **73**, 4278-4286 (1993).

[6] Y. Wang, M. Rivers, S. Sutton, P. Eng, G. Shen, and I. Getting, Rev. High Pressure Sci. Technol. **7**, 1490-1495 (1998).

[7] M.L. Rivers, T.S. Duffy, Y. Wang, P.J. Eng, S.R. Sutton, and G. Shen, in *Properties of Earth and Planetary Materials at High Pressure and Temperature*, edited by M.H. Manghnani and T. Yagi (American Geophysical Union, Washington, DC, 1998), Geophys. Monog. Ser. **101**, 79-86.

[8] M.S. Paterson and C.W. Weaver, J. Am. Ceram. Soc. **53**, 463-471 (1970).

[9] C.O. Hulse, S.M. Copley, and J.A. Pask, J. Am. Ceram. Soc. **46**, 317-323 (1963).

[10] G.L. Kinsland and W.A. Bassett, J. Appl. Phys. **48**, 978-984 (1977).

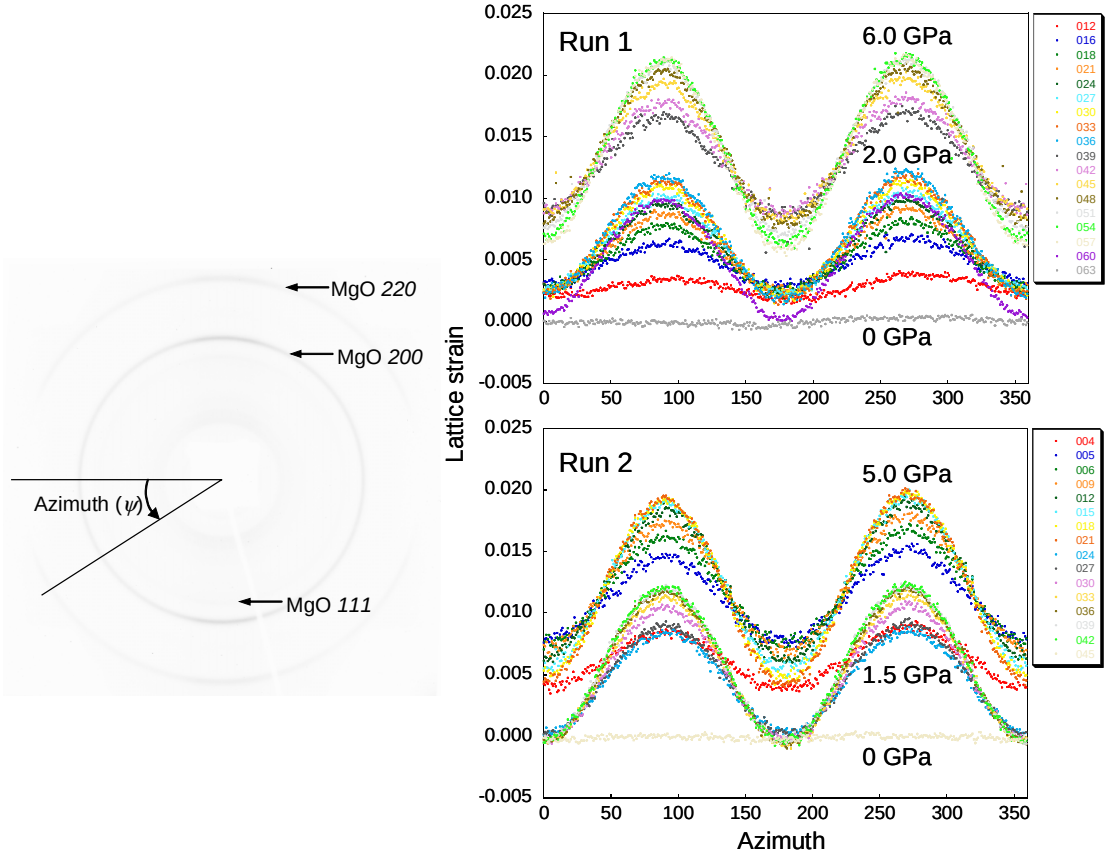

FIG. 2. Strain data on Mg(O 200) at pressures up to 6 GPa in run 1 (top) and run 2 (bottom). In the first run, data set 016 through 036 are collected at a pressure of 2.0 GPa, with the differential rams continuously advancing. The sample was then compressed isotropically to 6.0 GPa, and again, ram was advanced. Data set 063 was taken when a press load was released. In the second run, ram was advanced first at high pressure (5.0 GPa) and then at low pressure (1.5 GPa). Despite their different histories, both strain data are very consistent.

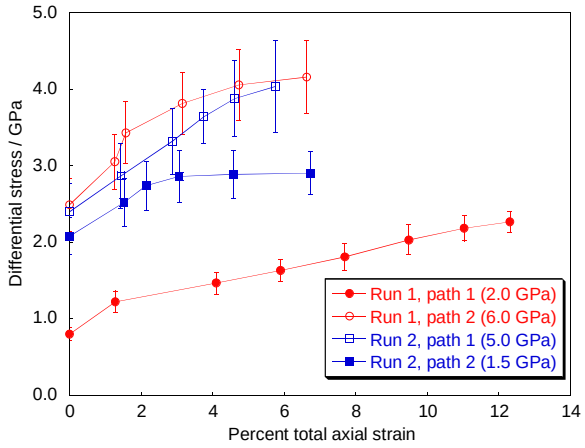

FIG. 3. Differential stress (Voigt-Reuss-Hill average) versus total axial strain for MgO. Error bar shows uncertainty estimated from Reuss and Voigt models.

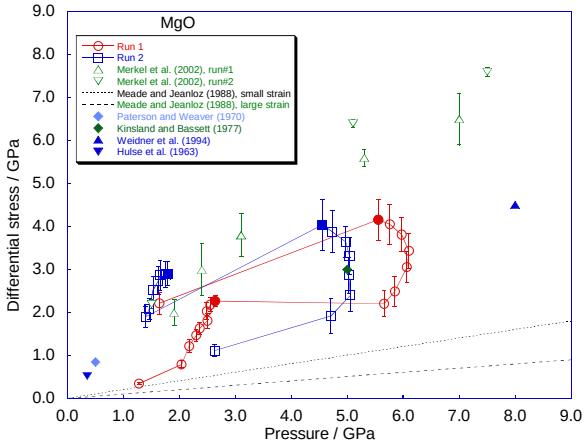

FIG. 4. Differential stress versus pressure for MgO. Open circles denote run 1, and open squares denote run 2. The last data point at each deformation process is shown by a solid symbol, indicating the lower bound of yield strength. Note that the capability of the D-DIA enabling differential stress increases at constant pressure.